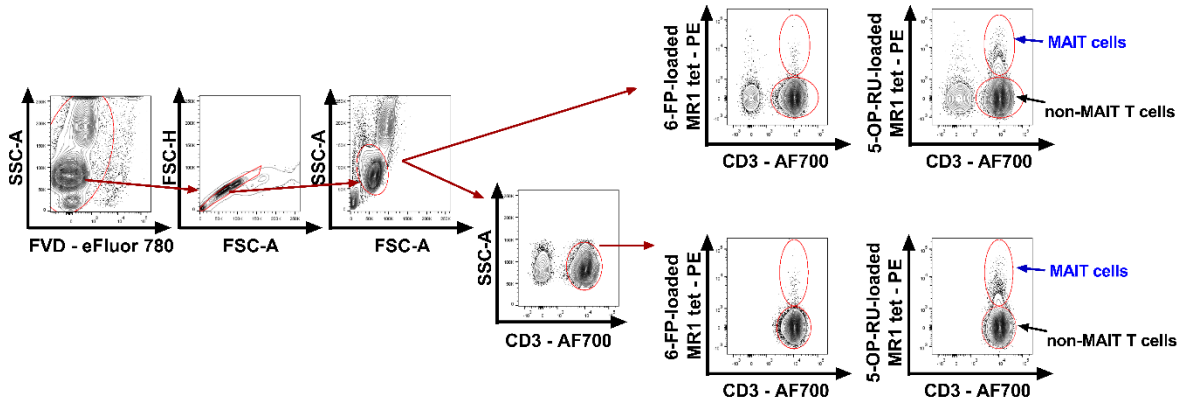

Supplementary Figure 1: Cytofluorimetric gating strategy to define peripheral blood MAIT and non-MAIT T cell populations. After excluding FVD^+ (fixable viability dye-positive) events, doublets were removed, and a lymphocyte gate was drawn based on forward and side scatter characteristics. MAIT cells were then defined as 5-OP-RU-loaded MR1 tetramer-positive cells among bulk lymphocytes or their $CD3^+$ fraction. MR1 tetramers loaded with 6-FP were used as a negative staining control to ensure precise gating.

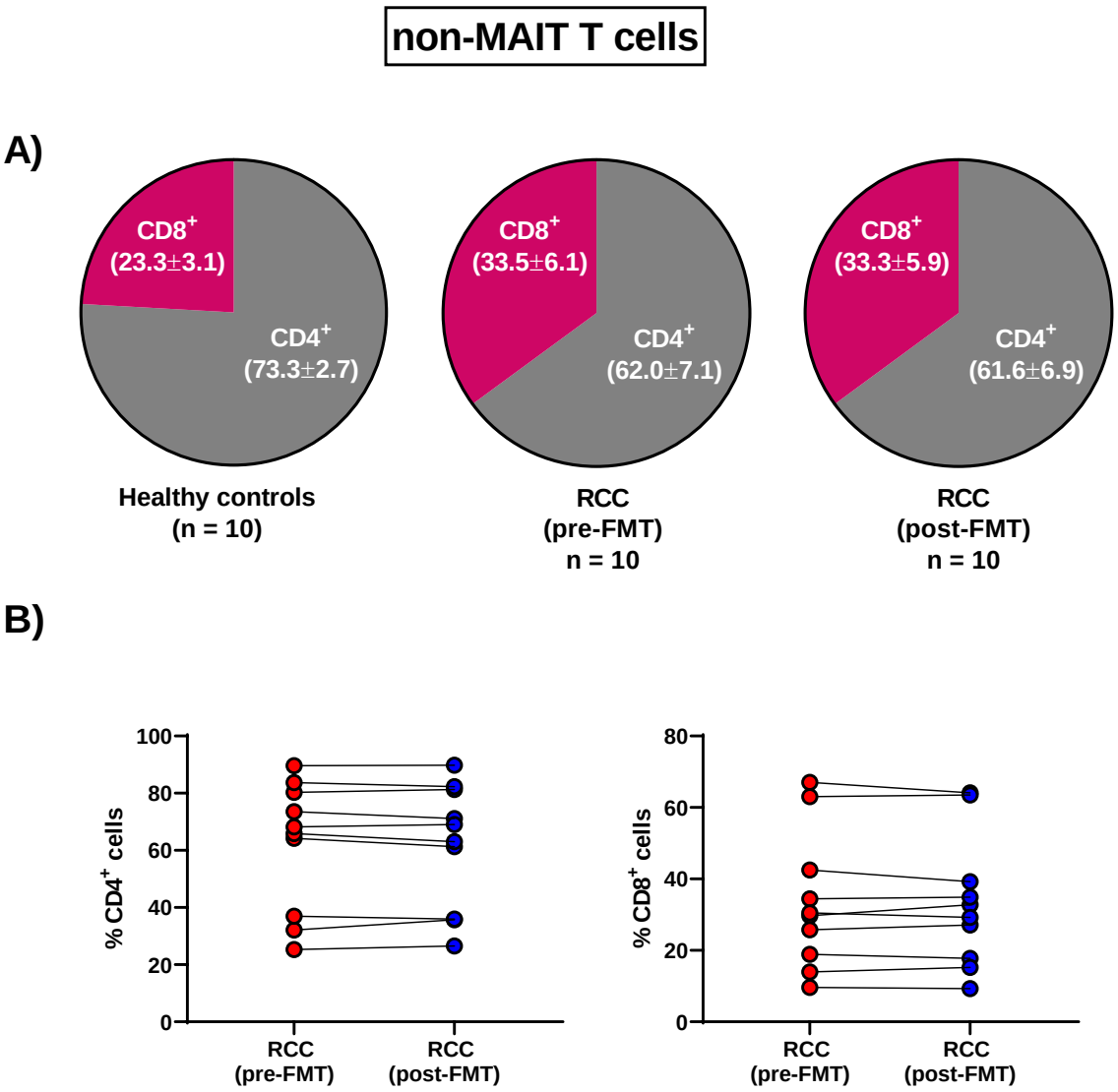

Supplementary Figure 2: FMT does not alter the frequencies of CD4$^+$ and CD8$^+$ non-MAIT T cells in the peripheral blood of RCC patients. The percentages of PB CD4$^+$ and CD8$^+$ cells were determined by flow cytometry among CD3$^+$ 5-OP-RU-loaded MR1 tetramer$^-$ (non-MAIT T) cells in 10 healthy controls (HCs) and 10 RCC patients before and after FMT. Pie charts illustrate the averaged distribution of non-MAIT T cells expressing CD4 or CD8 (A). Data are presented as mean ± SEM. No statistically significant differences were found using Mann-Whitney U tests (A) or Wilcoxon Signed Rank tests (B).

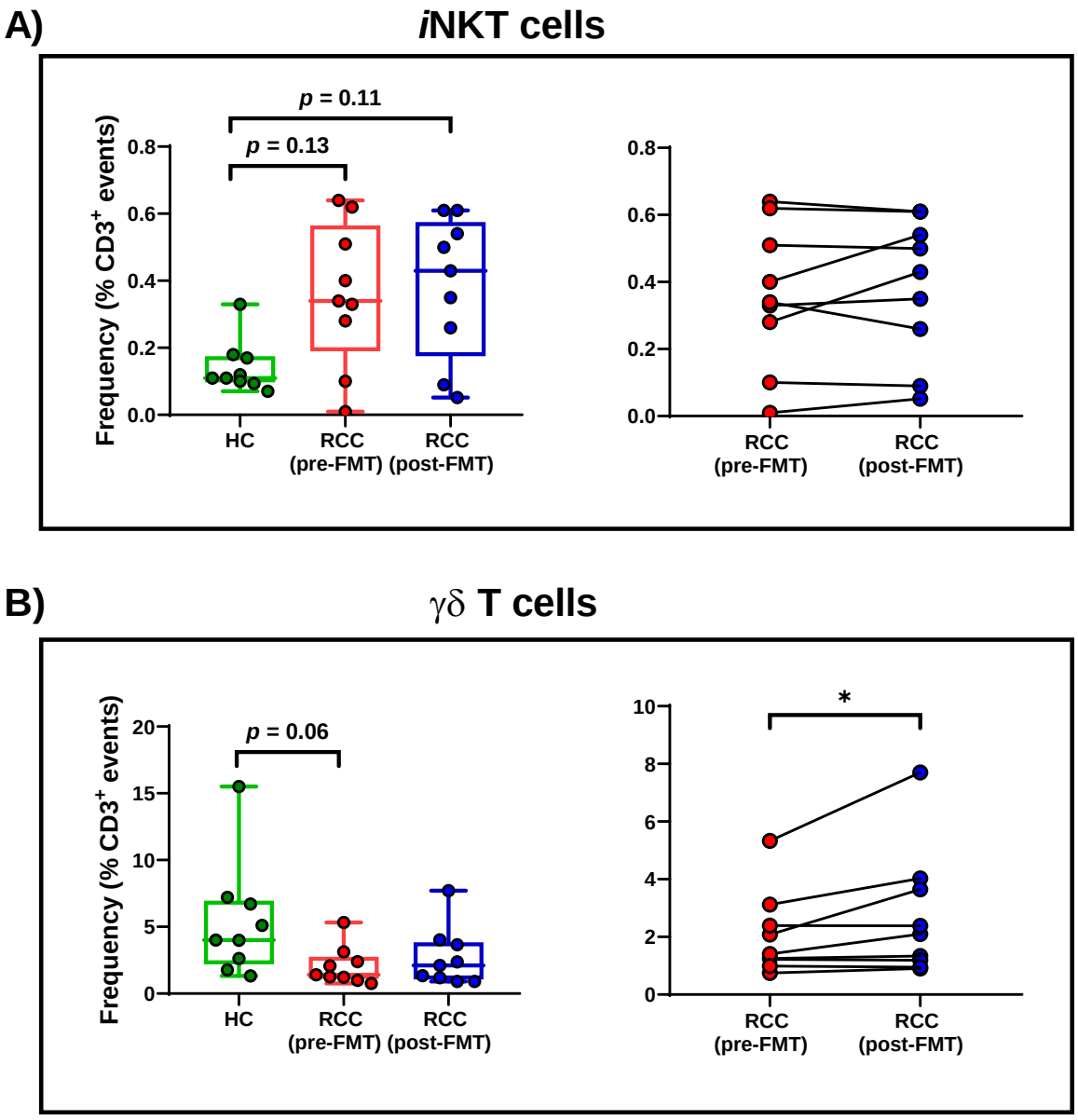

Supplementary Figure 3: FMT raises the peripheral blood frequencies of γδ T cells, but not *i*NKT cells, in RCC patients. The percentages of PBS-57-loaded CD1d tetramer$^+$ *i*NKT cells (A) and TCRγ/δ$^+$ γδ T cells (B) among CD3$^+$ events were determined by flow cytometry in the PB of nine healthy controls (HCs) and nine RCC patients before and 7 days after FMT. Each circle represents an individual sample. Statistical differences were computed using Kruskal-Wallis tests (followed by the Dunn's post-hoc test) for group comparisons (A-B, left panels), and using Wilcoxon Signed Rank tests for paired sample analyses (A-B, right panels). * denotes a significant difference with $p \leq 0.05$.

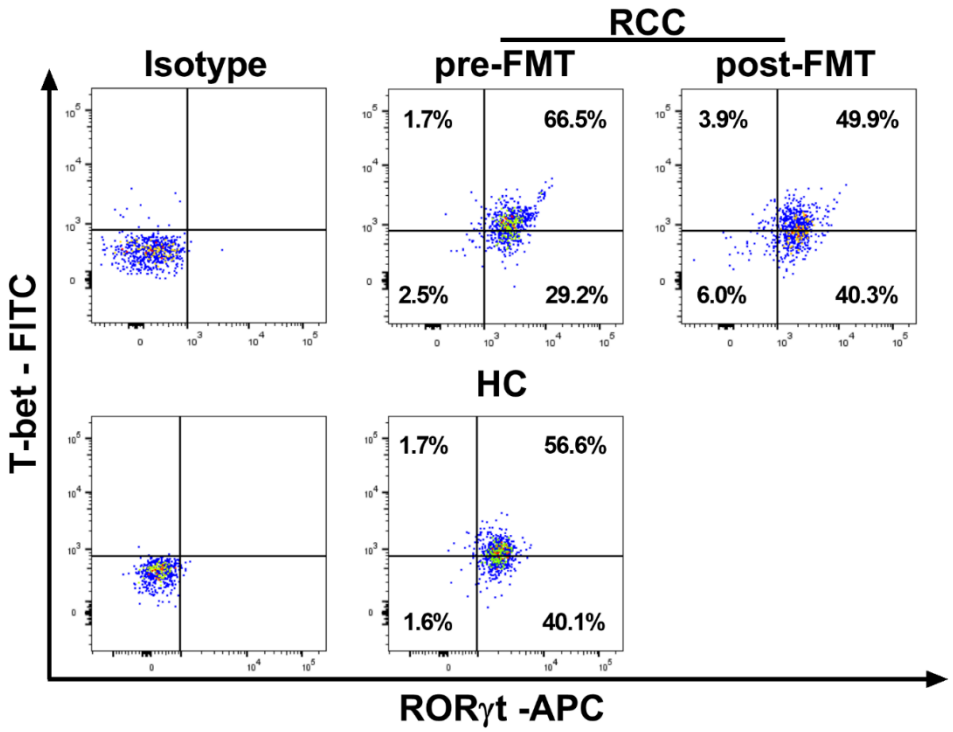

Supplementary Figure 4: Representative cytofluorimetric plots defining T-bet$^+$ and RORγt$^+$ MAIT cell subsets in the peripheral blood. PBMCs from a female healthy control (HC) blood donor and a female patient with RCC before and seven days after she received FMT were stained using mAbs to surface CD3, intracellular T-bet, intracellular RORγt, and MR1 tetramers as described in Materials and Methods. In separate tubes, cells were stained with isotype controls for anti-T-bet and anti-RORγt mAbs. After gating on CD3$^+$ 5-OP-RU-loaded MR1 tetramer$^+$ MAIT cells, the frequencies of T-bet$^+$RORγt$^-$, T-bet$^-$RORγt$^+$, T-bet$^+$RORγt$^+$ and T-bet$^-$RORγt$^-$ cells were determined by flow cytometry.

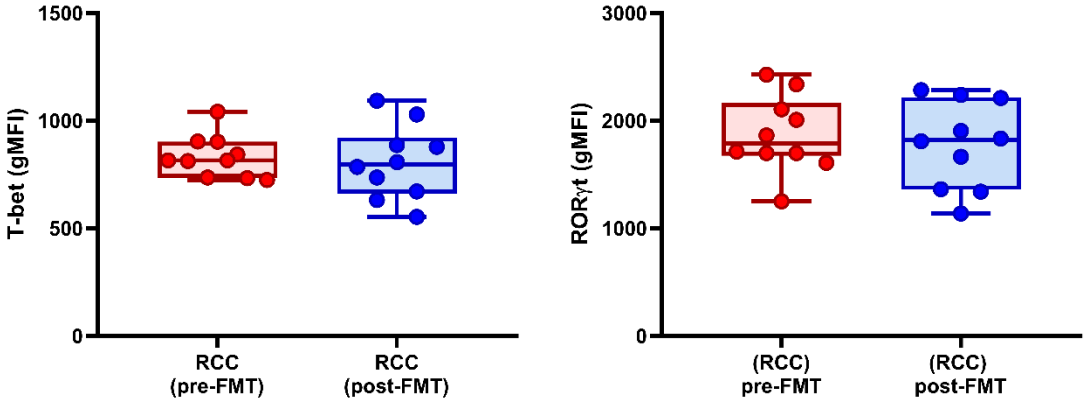

Supplementary Figure 5: FMT does not alter the expression of T-bet and RORγt on a per-MAIT cell basis. PBMCs from 10 RCC patients (before and seven days after FMT) were analysed by flow cytometry to determine the geometric mean fluorescence intensity (gMFI) of T-bet and RORγt among $CD3^+$ 5-OP-RU-loaded MR1 $tetramer^+$ MAIT cells.

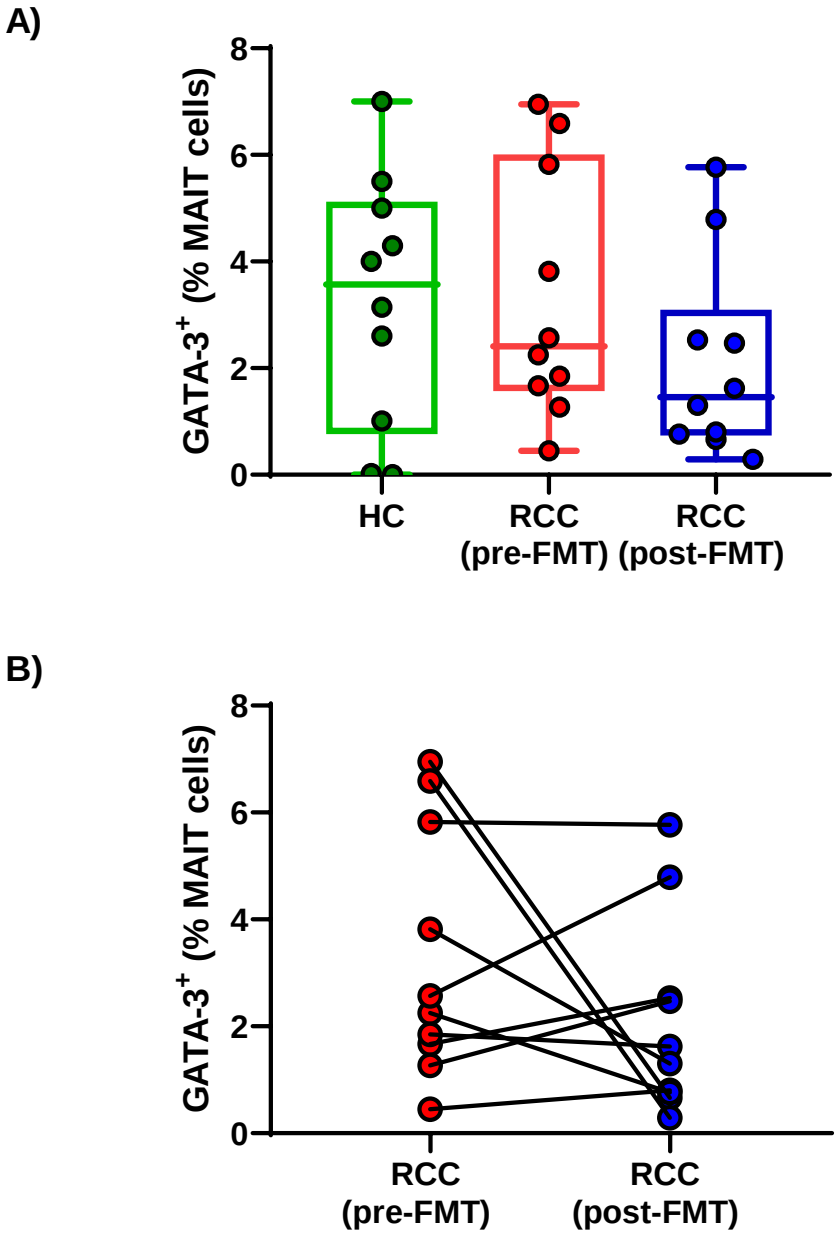

Supplementary Figure 6: FMT does not change the frequency of GATA-3$^+$ MAIT cells in RCC patients. Pre- and post-FMT PBMC samples from ten RCC patients as well as PBMCs from ten healthy controls (HCs) were analysed by flow cytometry for the expression of GATA-3 by CD3$^+$5-OP-RU-loaded MR1 tetramer$^+$ MAIT cells. Each circle represents an individual sample. No statistically significant differences were found using Kruskal-Wallis tests (followed by the Dunn's post-hoc test) (A) or Wilcoxon Signed Rank tests (B).

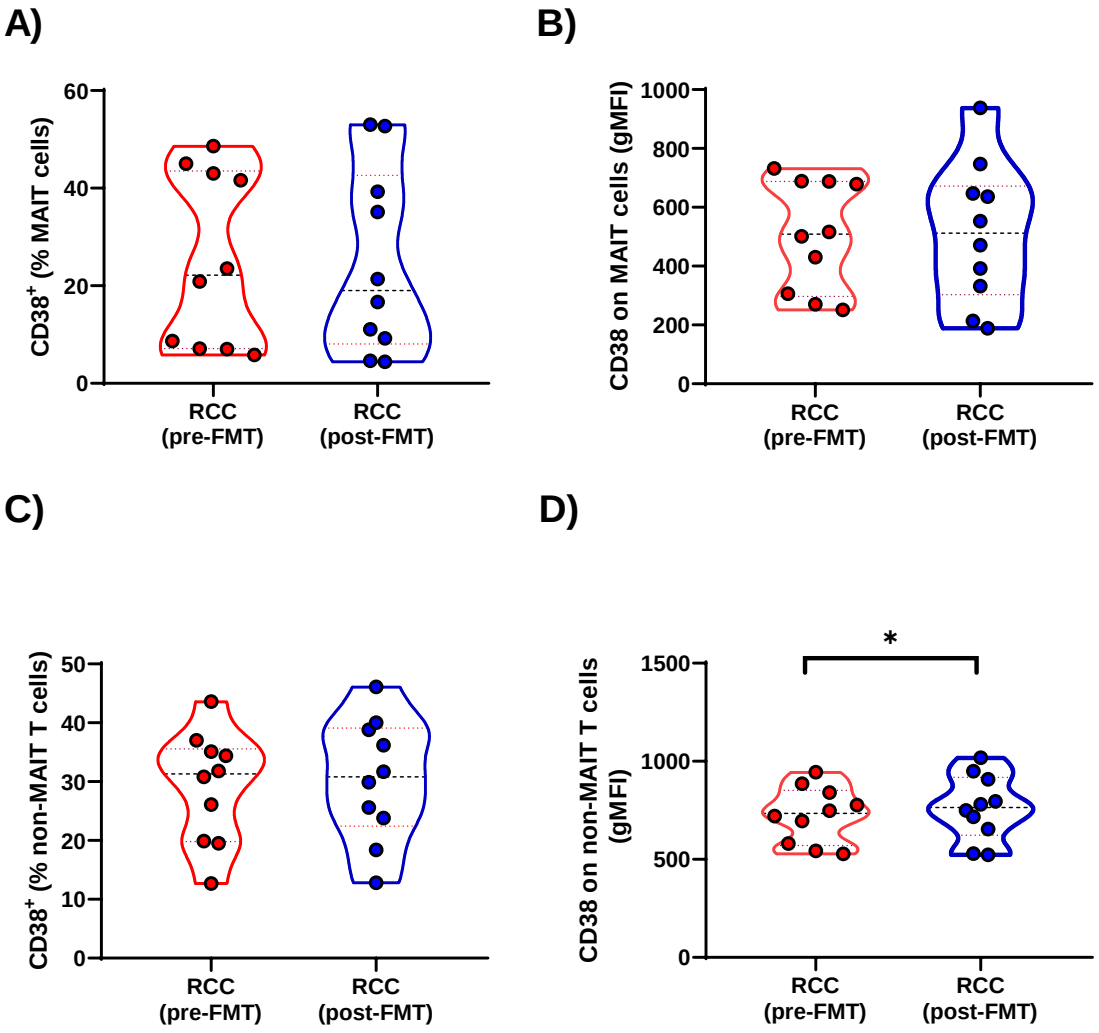

Supplementary Figure 7: FMT leads to a slight increase in CD38 expression by non-MAIT T cells. Pre- and post-FMT PBMC samples from ten RCC patients were analysed by flow cytometry for the expression of CD38 by MAIT ($CD3^+$5-OP-RU-loaded MR1 $tetramer^+$) cells (A-B) and non-MAIT T ($CD3^+$5-OP-RU-loaded MR1 $tetramer^-$) cells (C-D). Both the frequencies of $CD38^+$ cells (A and C) and the geometric mean fluorescence intensity (gMFI) of CD38 staining (B and D) are depicted. Paired *t*-tests were used to compare pre- and post-FMT values. * denotes a significant difference with $p \leq 0.05$.

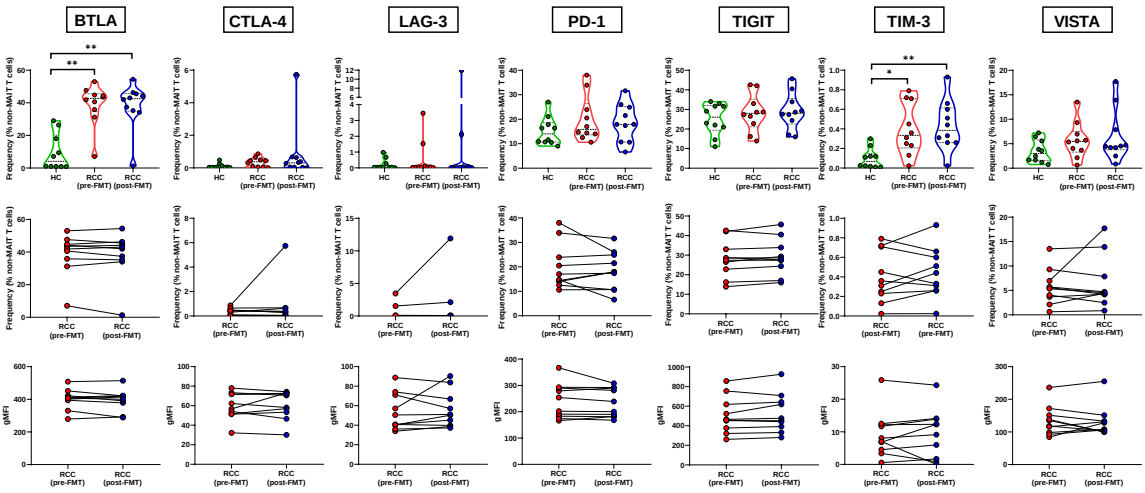

Supplementary Figure 8: FMT does not increase the expression of classic exhaustion/co-inhibitory markers on non-MAIT T cells. Pre- and post-FMT PBMC samples from ten RCC patients as well as PBMCs from ten healthy controls (HCs) were stained and interrogated by flow cytometry for the surface expression of BTLA, CTLA-4, LAG-3, PD-1, TIGIT, TIM-3 and VISTA by non-MAIT T lymphocytes defined as $CD3^+$ 5-OP-RU-loaded MR1 $tetramer^-$ cells. The percentages of cells expressing indicated markers are shown (top and middle rows), and so is the gMFI of staining for each marker (bottom row). Each circle represents an individual sample. Group comparisons (top row) were carried out using Kruskal-Wallis tests with the Dunn's post-hoc analysis. For paired sample comparisons (middle and bottom rows), the Wilcoxon Signed Rank test was used. * and ** denote significant differences with $p \leq 0.05$ and $p \leq 0.01$, respectively.

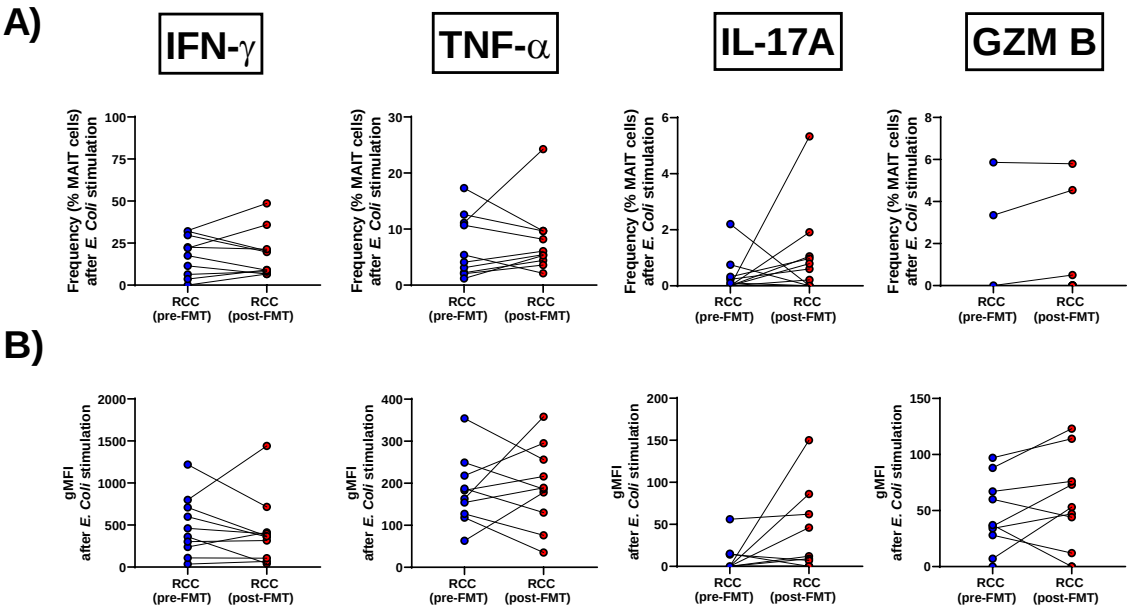

Supplementary Figure 9: MAIT cell responses to *E. coli* are comparable in pre- and post-FMT PBMC cultures. Pre- and post-FMT PBMCs from ten RCC patients were left untreated or stimulated for 24 hours with *E. coli* lysate followed by cytofluorimetric enumeration of IFN-γ^+, TNF-α^+, IL-17A$^+$ and GZM B$^+$ MAIT cells. The frequencies of cells expressing the above mediators (A) and their gMFI (B) are depicted. Background levels were obtained from unstimulated cultures and subtracted for each mediator. Paired sample comparisons were made using Wilcoxon Signed Rank tests (for IFN-γ, IL-17A and GZM B) and paired *t*-tests (for TNF-α).

RCC Patients		**Healthy Subjects**	
Age	Sex	Age	Sex
65	Male	65	Male
71	Male	70	Male
53	Male	53	Male
69	Male	67	Male
61	Male	61	Male
58	Male	60	Male
57	Male	56	Male
50	Male	48	Male
47	Female	44	Female
66	Female	67	Female

Supplementary Table 1. Age and sex of patients and healthy subjects enrolled in this study

Target	Fluorophore	Clone	Isotype	Reactivity	Supplier
BTLA	PE-Cy7	MIH26	mIgG2a, κ	human	BioLegend
CD3	APC-eFluor 780	UCHT1	mIgG1, κ	human	Thermo Fisher
CD3	Alexa Fluor700	UCHT1	mIgG1, κ	human	Thermo Fisher
CD3	PE-Cy7	UCHT1	mIgG1, κ	human	Thermo Fisher
CD4	Alexa Fluor 700	RPA-T4	mIgG1, κ	human	Thermo Fisher
CD8α	FITC	SK1	mIgG1, κ	human	Thermo Fisher
CD38	APC	HIT2	mIgG1, κ	human	Thermo Fisher
CD69	PE-Cy7	FN50	mIgG1, κ	human	Thermo Fisher
CTLA-4	PE-Cy7	14D3	mIgG2a, κ	human	Thermo Fisher
GATA-3	PE-eFlour 610	TWAJ	Rat IgG2b, κ	Human/mouse	Thermo Fisher
GZM B	Alexa Fluor 488	351927	mIgG2a	human	Invitrogen
IFN-γ	PE-Cy7	4S.B3	mIgG1, κ	human	Thermo Fisher
IL-17A	PerCP-Cy5.5	eBio64DEC17	mIgG1, κ	human	Thermo Fisher
LAG3	PE-eFluor 610	3DS223H	mIgG1, κ	human	Thermo Fisher
PD-1	FITC	MIH4	mIgG1, κ	human	Thermo Fisher
RORγt	APC	AFKJS-9	rat IgG2a, κ	human / mouse	Thermo Fisher
T-bet	FITC	4B10	mIgG1, κ	human / mouse	BioLegend
TCRγ/δ	PerCP-eFluor 710	B1.1	mIgG1, κ	human	Thermo Fisher
TIGIT	PerCP-eFluor 710	MBSA43	mIgG1, κ	human	Thermo Fisher
TIM-3	APC	F38-2E2	mIgG1, κ	human	Thermo Fisher
TNF-α	PE-eFluor 610	MAb11	mIgG1, κ	human	Thermo Fisher
VISTA	APC	B7H5DS8	mIgG1, κ	human	Thermo Fisher

Supplementary Table 2. Antibodies used for surface and intracellular staining in this study